

# Modelization of coordinated changes of adenylate energy charge and ATP/ADP ratio: application to energy metabolism in invertebrate and vertebrate skeletal muscle

*Modélisation des variations coordonnées de la charge énergétique adénylique et du rapport ATP/ADP : application au métabolisme énergétique du muscle squelettique des invertébrés et des vertébrés*

JEAN-PAUL RAFFIN <sup>(1)</sup>, MARIE-THÉRÈSE THÉBAULT <sup>(2)</sup>

<sup>(1)</sup> IFREMER, laboratoire de biotechnologie des micro-organismes hydrothermaux, BP 70, 29280 Plouzane Cedex, France.

<sup>(2)</sup> Collège de France, laboratoire de biologie marine, BP 225, 29182 Concarneau Cedex, France.

## RÉSUMÉ

Le régulation des variations coordonnées de la charge énergétique adénylique et du rapport ATP/ADP a été étudiée à l'aide d'une simulation par ordinateur. Si on considère que la réaction de l'adénylate kinase fonctionne à l'équilibre, il est possible de dériver une équation simple reliant ces 2 paramètres. La modélisation obtenue a permis l'analyse de l'incidence de la désamination de l'AMP sur la régulation du métabolisme énergétique cellulaire. ▲

**Mots clés :** charge énergétique adénylique, ATP/ADP, AMP désaminase, adénylate kinase.

## ABSTRACT

*Regulation of the coordinated adenylate energy charge (AEC) and ATP/ADP ratio variations was studied with the aid of computer-made simulations. When the equilibrium state for the adenylate kinase-catalyzed reaction has been assumed, the function describing the coordinated AEC and ATP/ADP ratio variations can be simply derived from the formulas describing these 2 parameters. The model was used to analyze incidence of AMP deamination in the coordinated regulation of cellular energy metabolism. ▲*

**Key words:** adenylate energy charge, ATP/ADP, AMP deaminase, adenylate kinase.

## VERSION ABRÉGÉE

Une formulation mathématique basée sur des transformations logarithmiques a été proposée pour rendre compte des interactions entre la charge énergétique adénylique (CEA) et le rapport ATP/ADP. Jusqu'à présent, cette analyse n'avait pas pris en compte les effets concomitants de la désamination de l'AMP ou des équilibres entre les espèces nucléotidiques libres et liées, composantes importantes du métabolisme musculaire. Nous avons effectué une simulation par ordinateur de l'évolution coordonnée de la CEA et du rapport ATP/ADP, en incluant ces paramètres.

Note présentée par Jean Rosa.

Note remise le 27 octobre 1995, acceptée après révision le 13 décembre 1995.

Corresponding author: J.-P. Raffin.

Les expériences de simulation ont généré des courbes dont la forme est dépendante de la constante d'équilibre de l'adénylate kinase (Keq) et non du taux de désamination de l'AMP ou de la fraction de nucléotides libres. Par contre, pour une consommation d'ATP donnée, le déplacement des points expérimentaux le long de cette courbe est fortement dépendant de tous ces paramètres. Il a ainsi été possible de calculer un effet tampon de la réaction de l'AMP désaminase qui était lié à la valeur de la constante d'équilibre de l'adénylate kinase, les pouvoirs tampons les plus élevés étant mesurés pour des valeurs plus importantes de la Keq. Nous avons dérivé une fonction décrivant les variations coordonnées de la CEA et du rapport ATP/ADP et dans laquelle apparaissait Keq :

$$\text{CEA} = \frac{x + 0.5}{x + 1 + \text{Keq}/x} \quad (x = \text{ATP/ADP})$$

Le modèle a été validé en superposant des valeurs expérimentales que nous avons obtenues au cours de l'exercice sur le muscle abdominal de *Palaemon serratus* (Crustacea; Decapoda), ainsi que des valeurs moyennes issues de la littérature sur 17 espèces de vertébrés et d'invertébrés.

Nos résultats montrent que les effets tampons de la réaction de l'AMP désaminase sur les variations des paramètres énergétiques sont surtout importants au début de l'exercice. De plus, ce pou-

**V**ariations in adenylate energy charge and ATP/ADP ratio, as well as phosphorylation potential, have been found to be regulated in a coordinated way which is dependent upon the current tissue energy demand [1]. It was shown that in a limited range of variations, a quasi-linear dependence between the logarithm of the energy charge value and the ATP/ADP ratio existed [1]. However, Reed's analysis was incomplete as it did not consider either the effect of concomitant AMP deamination, or distributions between bound and free nucleotide species – a problem which may be relatively easily solved by the contemporary NMR techniques.

To complete the above, we undertook studies in which the coordinated regulation of the adenylate energy charge and ATP/ADP ratio in response to various energy demand conditions was examined. In these studies, the effect of AMP deamination and the simultaneous variation of free and complexed adenylate species (free ADP and MgATP/ATP<sub>free</sub>) were taken into account (Fig. 1). The model was validated by using experimental data obtained from examination of crustacean tail muscle as well as similar data taken from literature fitted together to the theoretical simulation curve.

The results obtained enabled us to precise the physiological role of the AMP deaminase-catalyzed reaction, particularly in the dynamics of its action during the onset of energy ATP degradation, and to shed new light into the physiological meaning of the adenylate kinase equilibrium constant.

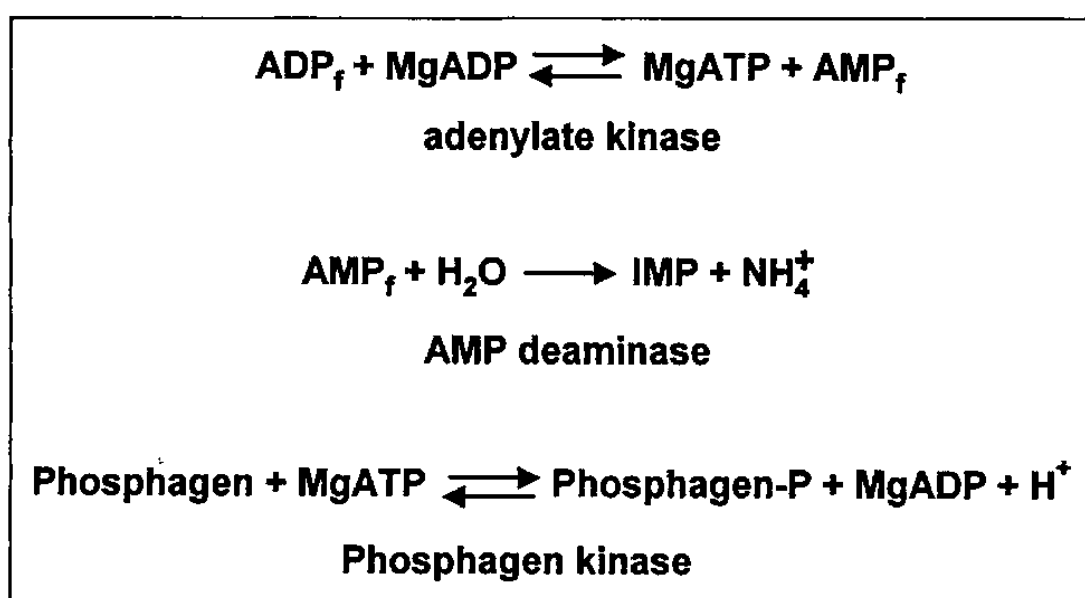


Figure 1. Reactions catalyzed by adenylate kinase, AMP deaminase and phosphagen kinase. *f* refers to free species.

voir tampon augmente au cours de la consommation d'énergie. L'AMP désaminase peut être considérée comme étant essentiellement un mécanisme permettant l'économie des réserves en phosphagènes et son action doit être considérée comme partie intégrante d'un système à 3 enzymes incluant l'adénylate kinase et la phosphagène kinase. Ainsi, l'efficacité de régulation par la désamination de l'AMP ne peut être optimale que si la constante d'équilibre de l'adénylate kinase est proche de 1. ▲

## Materials and methods

### Generation of the simulation curves

The simulations were made with the assumption of rapid adenylate nucleotides pool equilibration as a result of high adenylate kinase activity.

The algorithm used for simulation of the possible energetic parameter variations took into account effects dependent upon simultaneous AMP deamination and those connected with the specificity of adenylate kinase-catalyzed reaction (*i.e.* the concentrations of MgATP and free ADP) (Fig. 1). The concentrations of these 2 true adenylate kinase substrates have been assumed to be unchanged in the process of simulation.

### Experimental data

The values of adenylate energy charge and ATP/ADP ratio for crustacean (*Palaemon serratus*; Crustacea; Decapoda) abdominal muscle were determined both in the resting conditions as well as during intense exercise lasting 15 s, or longer until complete exhaustion.

The corresponding values for 16 other animal species listed in Table 1 were obtained from the literature.

## Results

### Simulation experiments in the presence of a fixed adenine nucleotide pool

The simulation curves presented in Figure 2 represent the coordinated response of the AEC and ATP/ADP ratio to different numerical values of the adenylate kinase-catalyzed reaction equilibrium constant (K<sub>eq</sub>). The curve number 4 on the Figure 2 represents that generated by the K<sub>eq</sub> value of 0.728, *i.e.* the mass action ratio determined for the *Palaemon serratus* muscle in resting conditions.

As may be seen from this figure, 2 different phases characterize the course of the each curve: the initial phase (significant ATP/ADP ratio changes and stable adenylate energy charge value) and the final phase (small ATP/ADP ratio changes but distinct energy charge variations).

The insert of Figure 2 represents the result of simulations as obtained by the linearization method of Reed [1]. Interestingly, a straight line-dependence has been produced only within the physiological range of adenylate kinase-catalyzed reaction equilibrium constant values.

Table I  
Adenylate energy charge and ATP/ADP values included into the experimental values

Species	AEC	ATP/ADP	References	Species	AEC	ATP/ADP	References
<b>Annelida</b>							
<i>Arenicola marina</i>				Horse			
Control	0.80	3.36	[8]	Control	0.95	8.97	[23]
12 h exercise	0.68	1.30		Exercise 6 m.s <sup>-1</sup>	0.94	8.39	
<i>Tubifex sp.</i>				Human			
Control	0.84	3.25	[9]	Control	0.94	8.20	
2 h exercise	0.74	2.06		Sub-maximal exercise	0.93	6.70	[24]
<b>Crustacea</b>				Human			
<i>Cherax destructor</i>				Control	0.94	7.15	
Control	0.93	7.90	[10]	Sub-maximal exercise	0.94	7.30	[25]
Exhausted	0.67	1.62		Maximal exercise	0.91	5.10	
<i>Crangon crangon</i>				Human			
Control	0.86	7.04		Control	0.94	7.65	
10 s exercise	0.81	4.62	[11]	12 s elec. stim. <sup>+</sup>	0.93	6.87	[26]
120 s exhaustion	0.56	1.18		52 s elec. stim. <sup>+</sup>	0.90	4.67	
<i>Orconectes limosus</i>				Human			
Control	0.94	9.98		Control	0.93	7.10	
27 ± 6 contractions	0.90	5.56	[12]	15 min exercise	0.92	6.09	[27]
66 ± 8 contractions	0.79	2.53		Exhausted	0.91	5.43	
<b>Insecta</b>				Human			
<i>Locusta migratoria</i>				Control	0.94	8.50	
Control	0.92	11.15	[13]	16 contractions	0.91	6.06	[28]
Jumping exercise	0.78	2.86		64 contractions	0.88	3.91	
<b>Mollusca</b>				Human			
<i>Argopecten irradians</i>				Control	0.95	10.68	
Control	0.94	6.66		22 s elec. stim. <sup>+</sup>	0.95	8.83	[29]
20-24 contractions	0.83	4.17	[14]	51 s elec. stim. <sup>+</sup>	0.90	4.64	
50-58 contractions	0.86	2.41		Human			
<i>Cardium tuberculatum</i>				Control	0.92	6.12	[30]
Control	0.92	7.23	[15]	Sub-maximal exercise	0.91	5.75	
41 ± 2 jumps	0.80	2.69		Human			
<i>Chlamys opercularis</i>				Control	0.94	8.45	[31]
Control	0.93	7.96	[16]	Exhausted	0.94	7.13	
Exhausted	0.33	0.44		Human			
<i>Loligo pealii</i>				Control	0.94	8.37	
Control	0.90	7.57	[17]	Sub-maximal exercise	0.94	7.59	[32]
Exhausted	0.52	0.96		Maximal exercise	0.92	5.32	
<i>Placopecten magellanicus</i>				Human			
Control	0.92	6.38	[18]	Control	0.94	7.87	[33]
Exhausted	0.77	2.37		Exhausted	0.92	5.46	
<b>Teleostei</b>				Rat			
<i>Oncorhynchus mykiss</i> *				Control	0.94	8.49	
Control	0.95	10.37		5 min contraction	0.87	3.86	[34]
Sustained exercise	0.95	9.66	[19]	20 min contraction	0.90	5.24	
Exhaustive exercise	0.82	2.52		Rat			
<i>Oncorhynchus mykiss</i> *				Control	0.94	8.43	
Control	0.94	8.31	[20]	60 s at 0.5 Hz	0.88	3.94	[35]
Exhausted	0.75	1.89		60 s at 1.0 Hz	0.81	2.03	
<i>Salvelinus fontinalis</i>				Rat			
Control	0.93	10.32	[21]	Control	0.89	5.19	[36]
<b>Mammalia</b>				Maximal exercise	0.73	2.25	
Dog							
Control	0.94	8.60	[22]				
Exhausted	0.91	5.90					

\* Former name: *Salmo-gairdneri*.  
+ elec. stim. = electrical stimulation.

### Effect of AMP deamination on the response curves

Figure 3 shows the coordinated changes of the 2 adenylate parameters (ATP/ADP ratio and adenylate energy charge), determined in the absence or in the presence of simultaneous AMP deamination, for 3 different adenylate kinase

equilibrium constants. For each value of the constant, the response curves were perfectly superposable, irrespective of AMP deamination. However, when the simulated drop of ATP concentration was up to 80%, the maximal range of adenylate parameters variation was affected by deamination of AMP in the way dependent upon the numerical

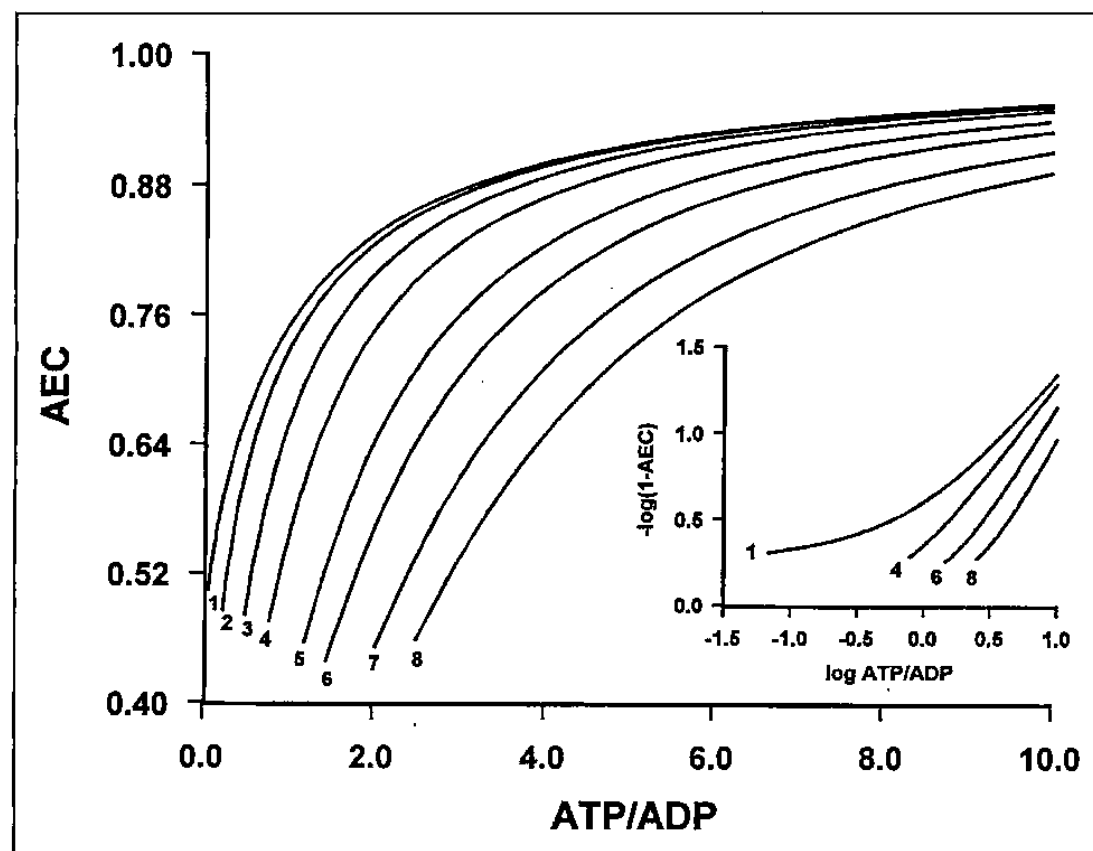


Figure 2. **Simulation of the coordinated changes of the adenylate energy charge (AEC) and the ATP/ADP ratio at different adenylate kinase equilibrium constants.** The concentration of the total adenylate pool was fixed at 5.565 mM (corresponding approximately to the value determined in young prawns [7]) and was assumed to be unchanged during the simulation process when AMP deaminase activity equalled 0. All the nucleotides were assumed to be accessible for the adenylate kinase-catalyzed reaction. The  $K_{eq}$  for adenylate kinase were  $4.17 \cdot 10^{-3}$  (1),  $6.76 \cdot 10^{-2}$  (2),  $2.87 \cdot 10^{-1}$  (3), 0.728 (4), 1.847 (5), 2.988 (6), 5.342 (7) and 7.795 (8). The  $K_{eq}$  of 0.728 is the mean mass action ratio measured, at rest, in the abdominal musculature of *Palaemon serratus*. (Insert) The insert shows the linearization proposed by Reed [1], for 4 of the simulation curves.

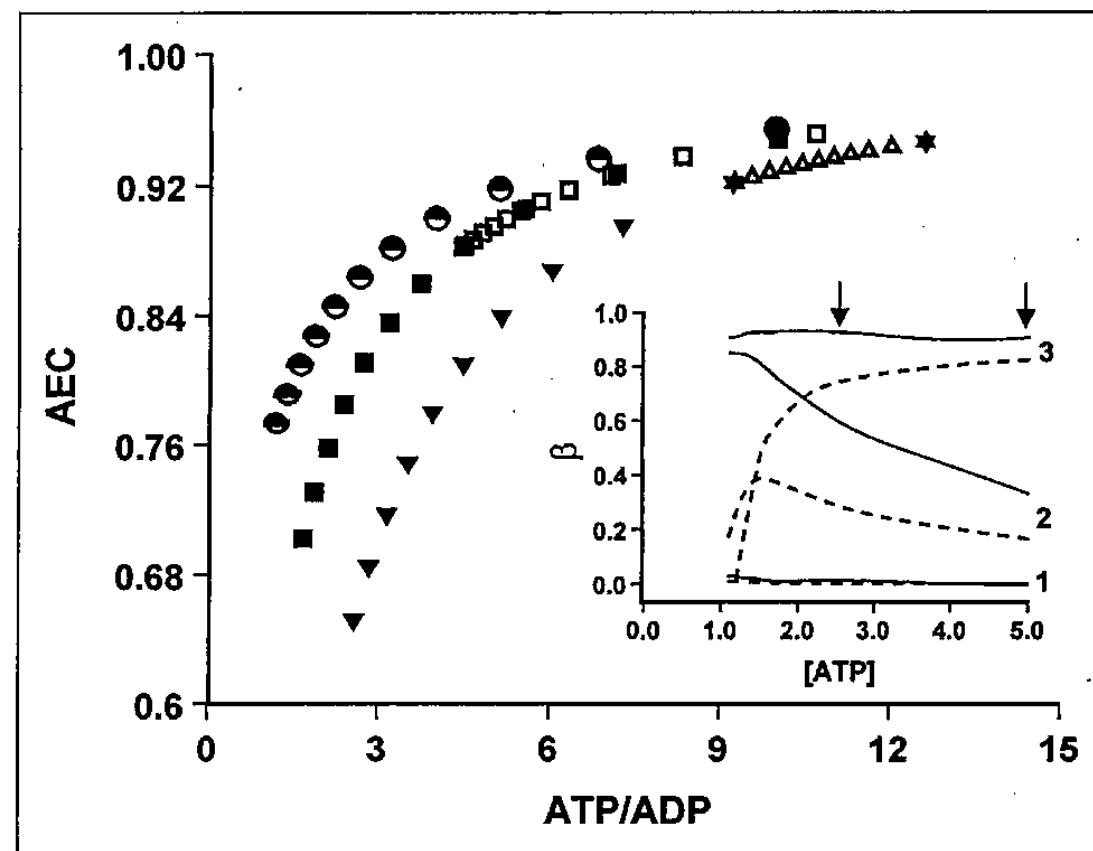


Figure 3. **Effect of AMP deamination on the coordinated changes of the adenylate energy charge (AEC) and the ATP/ADP ratio, at different adenylate kinase equilibrium constants.** The response curves show the variations of the parameters during a simulated decrease of up to 80% of the ATP concentration, in the absence (closed symbols) or presence (open symbols) of AMP deamination. The  $K_{eq}$  of the adenylate kinase were  $4.17 \cdot 10^{-3}$  (●, ○), 0.728 (■, □) and 2.988 (▼, △). (Insert) Calculation of the buffering effect of AMP deamination on variations of the adenylate energy charge (solid line) and the ATP/ADP ratio (dashed line) for different adenylate kinase equilibrium constants:  $4.17 \cdot 10^{-3}$  (1), 0.728 (2) and 2.988 (3). Arrows indicate the range of physiological adenylates variations.

value of the equilibrium constant. At low values of this constant, the changes observed were clearly less distinct and less dependent upon AMP deamination. At higher values of  $K_{eq}$  constant, however, the inhibitory effect of AMP deamination was very apparent. For quantitative evaluation of the observed buffering effect of AMP deaminase we used the following formula:

$$\beta_p = 1 - \left( \frac{\delta_{p(d)}}{\delta_{p(n)}} \right)$$

where p represents the adenylate parameter (energy charge or ATP/ADP ratio) value,  $\beta$  the strength of the buffering effect exerted on the parameter p, and  $\delta_{p(d)}$  and  $\delta_{p(n)}$  the appropriate differentials of the variations of p, both in the presence (d) or in the absence (n) of simultaneous AMP deamination, respectively. The numerical value of  $\beta$  was assumed to vary between 0 (no buffering effect) and 1 (maximal buffering effect).

The variations of  $\beta_{ATP/ADP}$  and  $\beta_{AEC}$ , expressed as a function of ATP concentration, are shown in the insert of Figure 3. In the normal physiological range of ATP concentration fluctuations (up to about a 50% decrease from the resting value), a numerical value of  $K_{eq} = 0.728$  gave roughly half of the maximum buffering effect possible. The value of index  $\beta$  increased continuously during the period of ATP consumption.

### Effect of nucleotide species compartmentation

The simulation curve presented in Figure 4 was generated with the following assumptions: either 10% concentration of free ADP, ATP complexed at 95% to  $Mg^{2+}$  and high AMP deaminase activity (conditions pertaining in vertebrate muscle); or 20% concentration of free ADP [2], ATP complexed at 85% to  $Mg^{2+}$  and no AMP deaminase activity (conditions pertaining in invertebrate muscle). The simulations were performed with the assumption that ATP consumption did not exceed 40% and that numerical value of the  $K_{eq}$  parameter was of 0.728.

When ATP consumption was initiated, the effects of the differences in the free ADP level on the response curve were rapidly damped. The shape of the simulated response curves was independent of the active nucleotide concentrations.

The response curve obtained showed 2 different regions of variations corresponding to the metabolic type of the vertebrate and invertebrate muscle, respectively. Also, the regions obtained corresponded respectively to the initial and final phases described above (Fig. 2).

### Modelling of the response curves

As it has been shown above, the shapes of the response curves depend exclusively on the adenylate kinase-cataly-

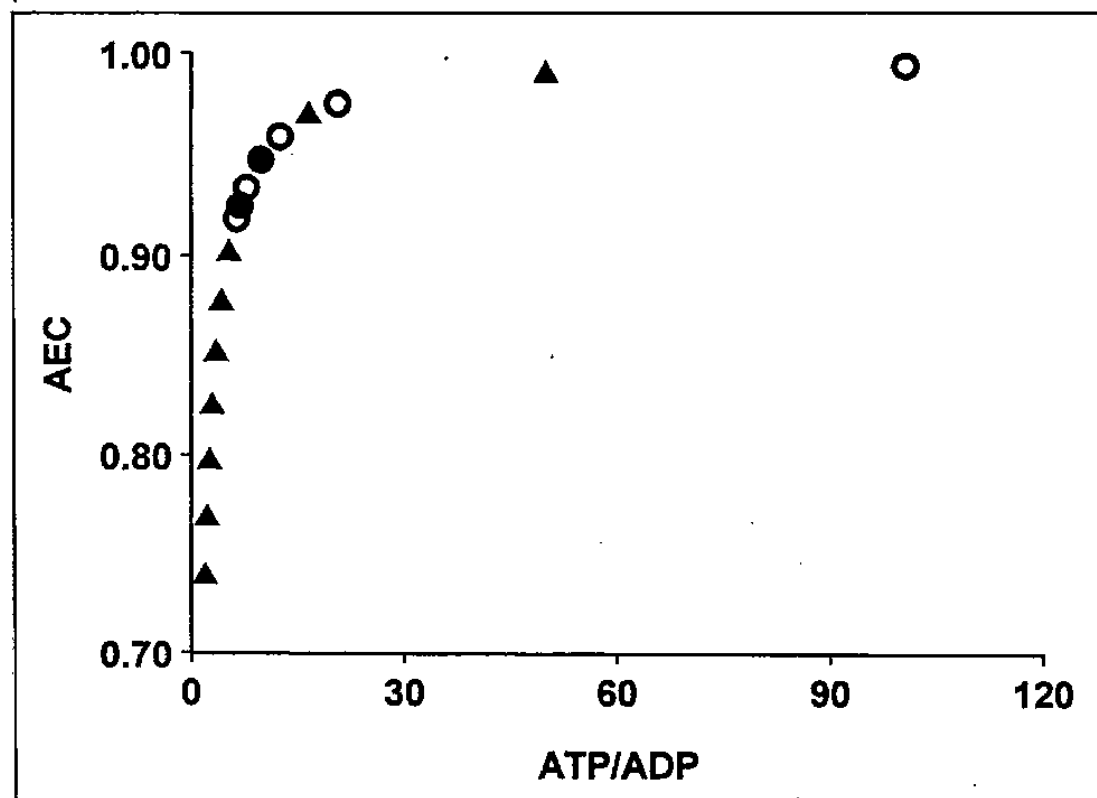


Figure 4. *Simulation of the coordinated changes of adenylate energy charge (AEC) and ATP/ADP ratio in the presence of different concentrations of MgATP, free ADP, at various levels of AMP deaminase activity. The assumed conditions are following: vertebrates (○): MgATP = 95%, ADP<sub>free</sub> = 10%, high activity of AMP deaminase; invertebrates (▲): MgATP = 85%, ADP<sub>free</sub> = 20%, no activity of AMP deaminase. The equilibrium constant of the adenylate kinase reaction was set to be equal to 0.728; the maximal decrease of the ATP concentration was assumed to be not higher than 40% of the total for each situation.*

zed reaction equilibrium constant (Keq), the numerical value of which can be easily estimated from the concentration of the different adenyl nucleotides species.

The equilibrium constant (Keq) of the adenylate kinase-catalyzed reaction is defined by following equation:

$$(1) \text{Keq} = \frac{\text{ATP} \cdot \text{AMP}}{\text{ADP}^2} = x \cdot \text{AMP/ADP}, \text{ where } x = \text{ATP/ADP}.$$

Inserting the value of  $x$  into the formula (2), describing the value of the adenylate energy charge (AEC):

$$(2) \text{AEC} = \frac{\text{ATP} + 1/2\text{ADP}}{\text{ATP} + \text{ADP} + \text{AMP}}$$

and dividing the each term of numerator and denominator by ADP, the equation (2) can be transformed into the form of equation (3):

$$(3) \text{AEC} = \frac{x + 0.5}{x + 1 + \text{Keq}/x}$$

#### Validation of the model with the experimental data

Figure 5 represents the mean experimental values of adenylate energy charge and ATP/ADP ratio, determined in resting and exercising muscle, of our own studies performed on *Palaemon serratus* tail muscle, or those performed on vertebrate or invertebrate muscle taken from literature (16 species). These data were fitted to the simulation curve generated for the Keq value of the adenylate kinase-catalyzed reaction equal 0.728.

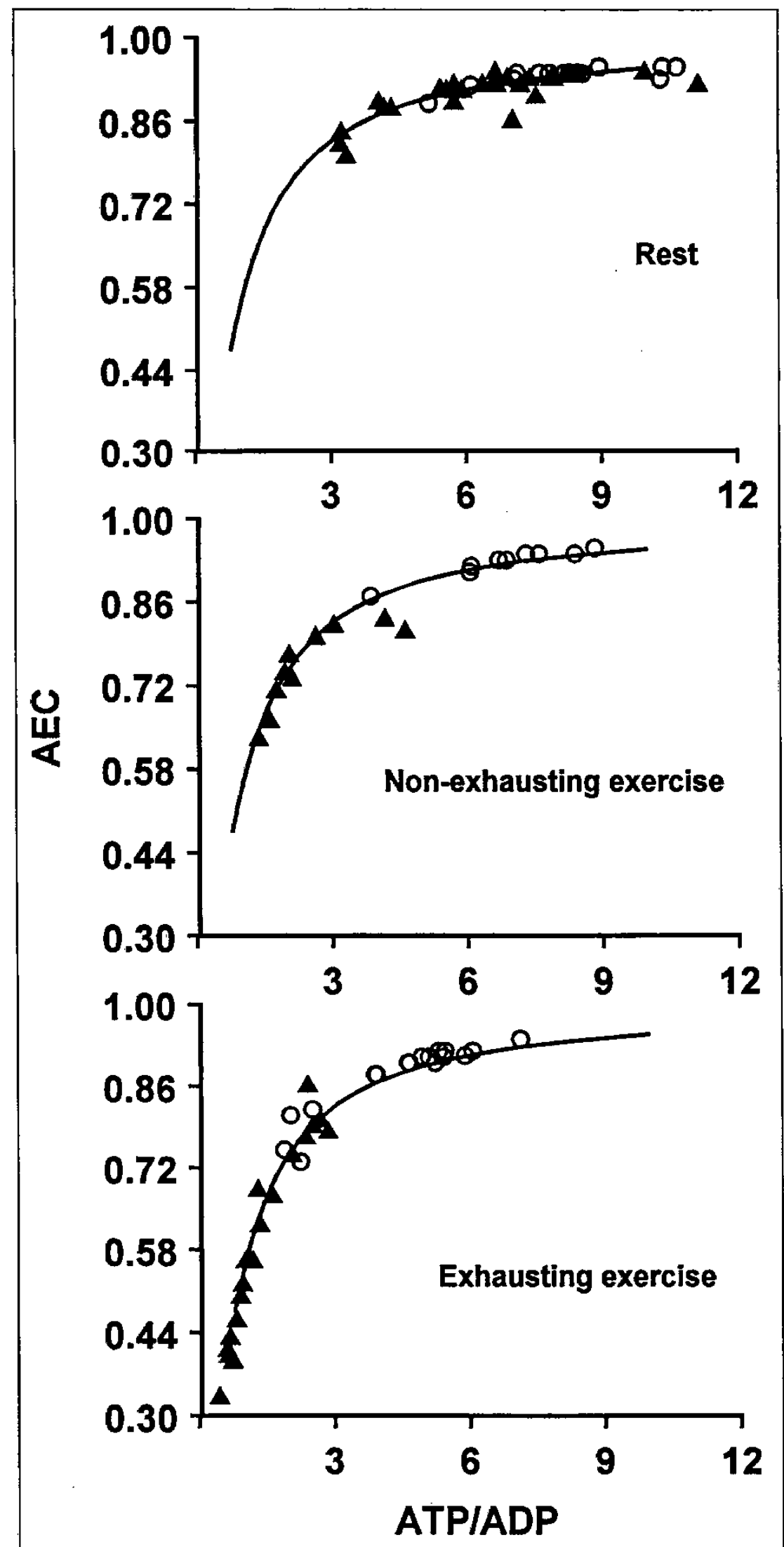


Figure 5. *Use of experimental values in the simulation curve. The theoretical curve was obtained for an adenylate kinase equilibrium constant of 0.728. ▲: mean values, from the literature (see Table I) for invertebrates, and our own experimental values on Palaemon serratus tail muscle. ○: mean values, from the literature, for vertebrates.*

As may be seen from the *Figure 5*, the buffering effect of adenylate deaminase was expressed mainly as an ATP/ADP ratio modulator, at rest. During exercise, AMP deaminase behaved progressively as an adenylate energy charge modulator.

The experimental data from vertebrate and invertebrate muscle fell into 1 of the 2 phases which could be distinguished through simulation (see *Fig. 4*).

## Discussion

The above derived equation describing coordinated variations of adenylate energy charge and ATP/ADP ratio did not need any logarithmic transformation [1]. The function described by this equation has rather a polynomial nature and is shown to depend exclusively on the numerical value of  $K_{eq}$  parameter. All other parameters tested (free/bound adenyl nucleotide species quotient, adenyl nucleotide pool size, extent of AMP deamination) did not influence the above function.

Even in the species displaying large variations of the adenylate parameters, the experimental data fit well with the theoretical simulation curve obtained for a given adenylate kinase  $K_{eq}$ , within the whole range of physiological ATP concentration variations (*Fig. 5*). This verifies positively the assumption that the reaction remains at equilibrium.

The role of AMP deaminase as a buffer of adenylate energy charge and ATP/ADP ratio variations in exercising muscle has been postulated a long time ago [3]. No one, however, had experimentally verified this postulate studying energetic metabolism of muscle taken from animals expressing a low activity of this enzyme.

The present study precises the dynamic pattern of the physiological regulation of AMP deamination in muscle.

At first, as described by Sahlin and Broberg [4], the reaction catalyzed by AMP deaminase buffers the ATP/ADP ratio changes (*Fig. 3*), but our results show that this function is important at the early period of exercise, *i.e.* when

the ATP/ADP ratio (in contrast to adenylate energy charge) responds sensitively to each change in ATP concentration. Secondly, the study strengthens that the buffering role of the enzyme towards the adenylate energy charge is not of equal importance during the whole period of ATP breakdown. Its importance increases dramatically with the decrease in ATP concentration, stabilizing the parameter during the period of exercise.

Thirdly, the indicatory significance of the ATP/ADP ratio is closely related with that represented by the Pcr/Cr ratio [5]. By analogy, the role of the AMP deaminase-catalyzed reaction may be considered as similar to that fulfilled by creatine kinase.

Fourthly, the significance of the AMP deaminase-catalyzed reaction may be regarded as a phosphagen sparing mechanism and the enzyme itself could be considered as an integral part of the 3-enzymes system composed from adenylate deaminase, adenylate kinase and phosphagen kinase (*Fig. 1*). The value of the *in vivo* adenylate kinase-catalyzed reaction corresponds well the requirement of the buffering role of the adenylate deaminase-catalyzed reaction (*Fig. 3*). As it has been shown by Kremien [6], the equilibrium constant of adenylate kinase-catalyzed reaction has to be equal one and the reaction itself to be at equilibrium to meet the maximal requirement of flexible regulation of the nucleotide pool. A maximal buffering capacity, which would have occurred for an adenylate equilibrium only 3 times higher than the *in vivo* value, would have resulted in an almost complete stabilization of the adenylate energy charge, the ATP/ADP ratio and, indirectly, the Pcr/Cr ratio. The consequence of the above can be an almost totally inefficient phosphagen kinase reaction, the only output of the system being the production of IMP. Conversely, a low value of the adenylate kinase-catalyzed reaction equilibrium constant, connected with a small AMP deaminase buffering effect, resemble the situation found in the muscle manifesting a very low AMP deaminase level, *i.e.* in invertebrate muscle or human pathology. In these conditions, the phosphagen kinase reaction remains the only ATP/ADP and adenylate energy charge buffer [5]. ▼

**Acknowledgements:** this study was supported by a grant from the Association française contre les myopathies. The authors would like to express their gratitude to Dr K. Kaletha, R. Malan and C. Leray for reading and discussing the manuscript.

## REFERENCES

1. Reed E.B. 1976. Coordination of adenylate energy charge and phosphorylation state during ischemia and under physiological conditions in rat liver and kidney. *Life Sci.* 19: 1307-22.
2. Thébault M.T., Raffin J.P., Pichon R. 1994. Cytosolic adenylate changes during exercise in prawn muscle. *C. R. Acad. Sci. Paris, Sér. III* 317: 991-5.
3. Chapman A.G., Atkinson D.E. 1973. Stabilization of the adenylate energy charge by the adenylate deaminase reaction. *J. Biol. Chem.* 248: 8309-12.
4. Sahlin K., Broberg S. 1990. Adenine nucleotide depletion in human muscle during exercise: causality and significance of AMP deamination. *Int. J. Sports Med.* 11: S62-7.
5. Kushmerick M.J. 1985. Patterns in mammalian muscle energetics. *J. Exp. Biol.* 115: 165-77.
6. Kremien A. 1976. Adenylate kinase reaction and energy charge. Application of statistical thermodynamic formalism to nucleotide pools. *Studia Biophys.* 59: 29-36.
7. Thébault M.T., Raffin J.P. 1991. Seasonal variations in *Palaemon serratus* abdominal muscle metabolism and performance during exercise, as studied by <sup>31</sup>P NMR. *Mar. Ecol. Progr. Ser.* 74: 175-81.
8. Surholt B. 1977. The influence of oxygen deficiency and electrical stimulation on the concentrations of ATP, ADP, AMP and phosphotaurocryamine in the body-wall of *Arenicola marina*. *Hoppe-Seyler's Z. Physiol. Chem.* 358: 1455-61.
9. Schöttler U. 1978. The influence of anaerobiosis on the levels of adenosine nucleotides and some glycolytic metabolites in *Tubifex sp.* (Annelida, Oligochaeta). *Comp. Biochem. Physiol.* 61B: 29-32.

10. England W.R., Baldwin J. 1983. Anaerobic energy metabolism in the tail musculature of the Australian yabby *Cherax destructor* (Crustacea, Decapoda, Parastacidae): role of phosphagens and anaerobic glycolysis during escape behavior. *Physiol. Zool.* 56: 614-22.
11. Onnen T., Zebe E. 1983. Energy metabolism in the tail muscles of the shrimp *Crangon crangon* during work and subsequent recovery. *Comp. Biochem. Physiol.* 74A: 833-8.
12. Gäde G. 1984. Effects of oxygen deprivation during anoxia and muscular work on the energy metabolism of the crayfish, *Orconectes limosus*. *Comp. Biochem. Physiol.* 77A: 495-502.
13. Gerez C., Kirsten R. 1965. Untersuchungen ueber ammoniakbildung bei der muskularbeit. *Biochem. Z.* 341: 534-42.
14. Chih C.P., Ellington W.R. 1983. Energy metabolism during contractile activity and environmental hypoxia in the phasic adductor muscle of the bay scallop *Argopecten irradians concentricus*. *Physiol. Zool.* 56: 623-31.
15. Meinardus-Hager G., Gebbott P.A., Gäde G. 1989. Regulatory steps of glycolysis during environmental anoxia and muscular work in the cockle, *Cardium tuberculatum*: control of low and high glycolytic flux. *J. Comp. Physiol. B* 159: 195-203.
16. Grieshaber M. 1978. Breakdown and formation of high-energy phosphates and octopine in the adductor muscle of the scallop, *Chlamys opercularis* (L.) during escape swimming and recovery. *J. Comp. Physiol.* 126: 269-76.
17. Storey K.B., Storey J.M. 1978. Energy metabolism in the mantle muscle of the squid *Loligo pealii*. *J. Comp. Physiol.* 123: 169-75.
18. De Zwaan A., Thompson R.J., Livingstone D.R. 1980. Physiological and biochemical aspects of the valve snap and the valve closure responses in the giant scallop *Placopecten magellanicus*. *J. Comp. Physiol.* 137: 105-14.
19. Parkhouse W.S., Dobson G.P., Hochachka P.W. 1988. Organization of energy provision in rainbow trout during exercise. *Am. J. Physiol.* 254: R302-9.
20. Pearson M.P., Spriet L.L., Stevens E.D. 1990. Effect of sprint training on swim performance and white muscle metabolism during exercise and recovery in rainbow trout (*Salmo gairdneri*). *J. Exp. Biol.* 149: 45-60.
21. Walesby N.J., Johnston I.A. 1980. Temperature acclimation in brook trout muscle: adenine nucleotide concentrations, phosphorylation state and adenylate energy charge. *J. Comp. Physiol. B* 139: 127-33.
22. Brzezinska Z. 1987. Muscle metabolism during prolonged physical exercise in dogs. *Arch. Int. Physiol. Biochim.* 95: 305-12.
23. Harris R.C., Marlin D.J., Snow D.H., Harkness R.A. 1991. Muscle ATP loss and lactate accumulation at different work intensities in the exercising thoroughbred horse. *Eur. J. Appl. Physiol.* 62: 235-44.
24. Sahlin K., Palmskog G., Hultman E. 1978. Adenine nucleotide and IMP contents of the quadriceps muscle in man after exercise. *Pflügers Arch.-Eur. J. Physiol.* 374: 193-8.
25. Katz A., Broberg S., Sahlin K., Wahren J. 1986. Muscle ammonia and amino acid metabolism during dynamic exercise in man. *Clin. Physiol.* 6: 365-79.
26. Chasiotis D., Bergström M., Hultman E. 1987. ATP utilization and force during intermittent and continuous muscle contractions. *J. Appl. Physiol.* 63: 167-74.
27. Norman B., Sollevi A., Kaijser L., Jansson E. 1987. ATP breakdown products in human skeletal muscle during prolonged exercise to exhaustion. *Clin. Physiol.* 7: 503-9.
28. Spriet L.L., Söderlund K., Bergström M., Hultman E. 1987. Anaerobic energy release in skeletal muscle during electrical stimulation in men. *J. Appl. Physiol.* 62: 611-5.
29. Bergström M., Hultman E. 1988. Energy cost and fatigue during intermittent electrical stimulation of human skeletal muscle. *J. Appl. Physiol.* 65: 1500-5.
30. Norman B., Sollevi A., Jansson E. 1988. Increased IMP content in glycogen-depleted muscle fibres during submaximal exercise in man. *Acta Physiol. Scand.* 133: 97-100.
31. Broberg S., Sahlin K. 1989. Adenine nucleotide degradation in human skeletal muscle during prolonged exercise. *J. Appl. Physiol.* 67: 116-22.
32. Sahlin K., Broberg S., Ren J.M. 1989. Formation of inosine monophosphate (IMP) in human skeletal muscle during incremental dynamic exercise. *Acta Physiol. Scand.* 136: 193-8.
33. Sahlin K., Ren J.M. 1989. Relationship of contraction capacity to metabolic changes during recovery from a fatiguing contraction. *J. Appl. Physiol.* 67: 648-54.
34. Spriet L.L., Matsos C.G., Peters S.J., Heigenhauser G.J.F., Jones N.L. 1985. Muscle metabolism and performance in perfused rat hindquarter during heavy exercise. *Am. J. Physiol.* 248: C109-18.
35. Spriet L.L. 1989. ATP utilization and provision in fast-twitch skeletal muscle during tetanic contractions. *Am. J. Physiol.* 257: E595-605.
36. Weicker H., Hageloch W., Luo J., Müller D., Werle E., Sehling K.M. 1990. Purine nucleotides and AMP deamination during maximal and endurance swimming exercise in heart and skeletal muscle of rats. *Int. J. Sports Med.* 11: S68-77.